Finite Element Analysis of Flexural Strengthening of Reinforced Concrete Beams Using Near-Surface Mounted CFRP Rebars

Aaditya Agrahari*[1], Jayaprakash J[2]

[1]Undergraduate Student, School of Civil Engineering, Vellore Institute of Technology, Vellore, India

[2]Professor, Department of Structural & Geotechnical Engineering, Vellore Institute of Technology, Vellore, India

*Email: aadityaagrahari99@gmail.com

Abstract

Most of the standing structures today have already deteriorated or are on the verge of deterioration due to an increase in their age and harsh environmental conditions. For this very reason, the structures are in need of being upgraded or replaced. Retrofitting using near-surface mounted (NSM) fiber-reinforced polymer (FRP) rods has now emerged as a promising technique for strengthening the reinforced concrete members by increasing their flexural strength. This study aims to numerically investigate the efficiency of the NSM technique for flexural strengthening of RC beams by using finite element (FE) software, ABAQUS, and also evaluate the impact of variables such as concrete strength, embedded length of FRP rods, filler material used for the FRP rods, and the number of FRP rods provided. Validation of the finite element model was confirmed by first making a comparison with the experimental study presented in the literature for an un-strengthened beam. Thereafter, the validated model was used to simulate reinforced concrete beams strengthened with the NSM technique. The numerical results of the cracking moment, steel yielding moment, ultimate bending moment, and deflection at failure were reported and the impact of the variables was evaluated. The FE analysis results indicated that for the RC beams strengthened with NSM FRP rods, the flexural capacity significantly increased compared to the control beam, while the mid-span deflections of strengthened beams at failure decreased compared to the control beam.

Keywords: *Near-surface mounted (NSM) Fibre-reinforced polymer (FRP); Numerical Modelling; Flexural Strengthening; Finite Element Analysis; Reinforced Concrete (RC) Beams; Ultimate Bending Moment.*

1. Introduction

Once a structure is constructed, it goes into a constant process of deterioration from the very first day. Most of the standing structures today have already deteriorated due to an increase in their age and harsh environmental conditions. These structures are in poor condition, not solely due to deterioration processes, but also due to many different factors, such as adverse environmental conditions that cause the corrosion of reinforcements, physical damage, and many more. There can be errors made during design and execution, as well as when there is a change in the load-carrying capacity requirement for the structure, overloading, or change in function of the structure. These structures can be made to stand intact and last a long-time using retrofitting techniques. To overcome all these limitations, the use of near-surface mounted fiber-reinforced polymer rods as a retrofitting technique is a promising option. The use of near-surface mounted (NSM) fiber-reinforced polymers (FRP) has stood out as an innovative technique to strengthen reinforced concrete members by increasing their flexural strength. As this technology of Near-Surface Mounted Fiber-Reinforced Polymer reinforcement strengthening emerges, the structural behavior of RC elements strengthened with NSM FRP rebars needs to be investigated. Although innumerable experimental studies have been conducted on the problem of strengthening and retrofitting reinforced concrete beams with FRP composites, further numerical, analytical, and experimental studies are needed to deeply clarify the effects of different factors on the formation of different failure modes, ultimate carrying capacity, ultimate deflection, and many more. Hence, a

thorough investigation is needed to find out the effects of these variables. The finite element analysis method can be used to study the behavior of the concrete and reinforcements, which allows a clear understanding of how the strengthened member would react to an actual loading scenario.

2. Literature Review

Retrofitting using near-surface mounted fiber-reinforced polymer (FRP) rods has now emerged as a promising technique, along with the externally bonded FRP laminates, for strengthening the reinforced concrete members by increasing the flexural and shear strength (Lorenzis et.al. 2001). The use of FRP material is preferred compared to conventional materials; steel because of its remarkable characteristics such as high strength to weight ratio, high resistance to corrosion, and an appropriate degree of durability (Lorenzis et.al. 2002). It is one of the most impressive techniques to increase the ultimate sustainable load capacity of existing reinforced concrete structures. In this method, a groove is cut in the desired direction into the concrete surface. The groove is then filled halfway with epoxy paste and the FRP rod is placed in the groove and lightly pressed. This forces the paste to flow around the rod and fill the spaces between the rod and the sides of the groove. The groove is then filled with more paste and the surface is levelled (Lorenzis et.al. 2000). One of the many advantages of this technique is that, FRP rods used are protected by the concrete cover, making them less vulnerable to accidental impact and mechanical damage, fire, and vandalism. The amount of site installation work can be greatly reduced since no surface preparation is required other than the grooving (Al-Mahmoud et.al. 2009).

An investigation on the effectiveness of NSM FRP rods as a strengthening system for RC elements was done by Lorenzis et.al. (2000) which suggested that the NSM FRP rods could increase the load capacity by approximately 47.64% compared to a non-strengthened beam. However, this was accompanied by some reduction in ductility and undesirable concrete cover separation failure. Abdzaid and Kamonna (2019) investigated cracking and ultimate loads, crack width, displacement, and failure modes for beams strengthened with the NSM technique. They found that the beams achieved a significant enhancement in ultimate flexural strength by approximately 108% relative to the control beam. NSM FRP rods can be used to significantly increase the shear capacity of RC elements, with an efficiency that varies depending on the tested variables (Lorenzis and Nanni, 2001). NSM bars reinforcement improves the performances of the strengthened beams in terms of failure load and ductility when compared to the beams strengthened with an equivalent amount of EBR reinforcement (F. Ceroni, 2010). The behavior of reinforced concrete flexural beams strengthened with FRP rods through the NSM method using parametric analysis on validated specimens was investigated which suggested that the load-carrying capacity of beams strengthened with CFRP was found to be higher than that of beams strengthened with GFRP, and AFRP, while the ultimate deflection of strengthened beams was relatively independent of the FRP materials (Panahi and Izadinia, 2018).

Al-Mahmoud et. al. (2009) investigated the possibility of using CFRP rods to strengthen concrete structural members with the NSM technique by performing macro-finite-element (MFE) analysis to calculate the deflection at different stages of the response and to build the global load-deflection curve of a structural member. The existing analytical models already used in standard RC beams showed a strong correlation with the experimental results in terms of the load-deflection curve. Bond tests on 8 mm diameter carbon bars performed by De Lorenzis et al. (2002) demonstrated that ultimate loads increase almost linearly with bond length when between 40–180 mm. Sharaky et. al. (2014) did a comparison of strengthened and control beams that showed enhancement of 155.8% and 129.8% in the yielding loads, while the increase in the ultimate loads was 166.3% and 159.4% for beams strengthened with carbon fiber-reinforced polymer (CFRP) and glass fiber reinforced polymer (GFRP), respectively. The beams strengthened with CFRP bars experienced higher stiffness than the corresponding beams

with GFRP bars. Bond tests performed by Seracino et al. (2007) on carbon strips showed that the ultimate load does not increase any further for a bond length longer than 200 mm.

Hassan and Rizkalla (2004) tested and found that development lengths should not be less than 80 times the bar diameter to ensure proper bond strength and to limit free-end slip. Experimental study on the bond between NSM FRP rods and concrete and factors affecting bond performance suggests that the surface configuration of the FRP rods influences the bond strength, as deformed rods appear to be more efficient than sandblasted rods from the standpoint of bond performance, also increasing the groove size, and thus the cover thickness, which leads to higher bond strength. (Lorenzis and Nanni 2002). The bond mechanism of NSM FRP bars used for flexural strengthening of concrete structures strengthened with limited bond lengths suggested that the development length of NSM CFRP bars should not be less than 80 times their diameter while changing the type of epoxy adhesive seemed to have only a negligible effect on the ultimate load capacity of the strengthened beams (Hassan et. al. 2004). The bond tests performed on carbon strips showed that the ultimate load does not increase any further for a bond length longer than 200 mm (Seracino et. al. 2007).

3. Experimental Setup

The finite analysis of this study is based on the experimental research of Al-Mahmoud et al. (2009) on the reinforced concrete beam strengthened with NSM FRP bars. In this study, the effects of NSM FRP rods on the ultimate flexural capacities and load-deflection curves of nine strengthened beams with different geometrical and material properties were compared with a control beam that was un-strengthened. The simulation of the flexural behavior of reinforced concrete beams strengthened with NSM FRP composites is done using the finite element software ABAQUS. The study first seeks to validates the finite element simulation work by making a comparison with the experimental study from literature work by Al-Mahmoud et al. (2009) for un-strengthened beam. And finally, the research work investigates the effects of the flexural capacities of the strengthened beams by changing the variables specifications such as concrete strength, embedded length of FRP rods, filler material used for the FRP rods, and number of FRP rods adopted. The study makes the comparison by accessing the bending moment versus the mid-span deflection graph, the concrete, cracking moment, steel yielding moment, ultimate bending moment, and deflection at failure.

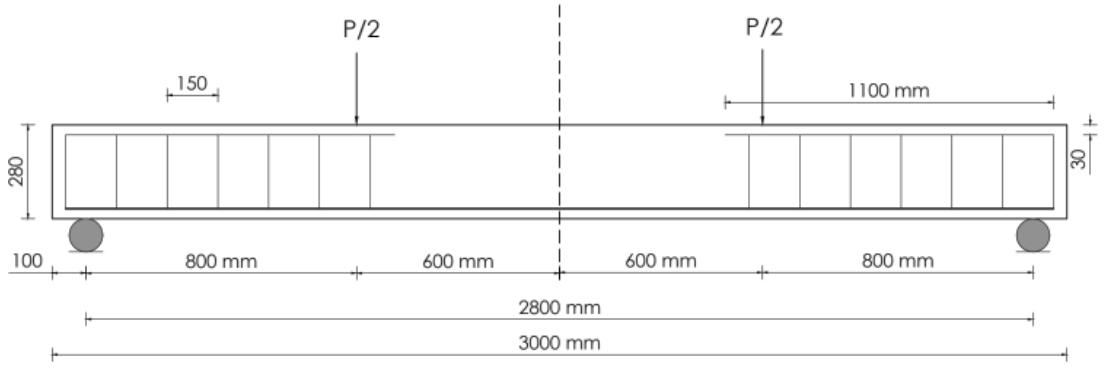

Figure - 1: Longitudinal Profile of Reinforced Control Beam used

As seen in figure-1 above, the total length of the beam was 3000 mm, with a center-to-center length of 2800 mm in between supports. The two-point loads were applied at a distance of 800 mm from the supports. The reinforced concrete beams had rectangular section dimensions of 280 mm × 150 mm,

with reinforcements of 2Φ12, and 2Φ6 in the tension and compression zones, respectively. As seen in fig. 2, the steel stirrups were provided at a spacing of Φ6 @ 150 mm. The strengthened beams were provided with either a single 12 mm diameter FRP at the center or two 6 mm diameter FRPs as shown in figure 2 & figure 3.

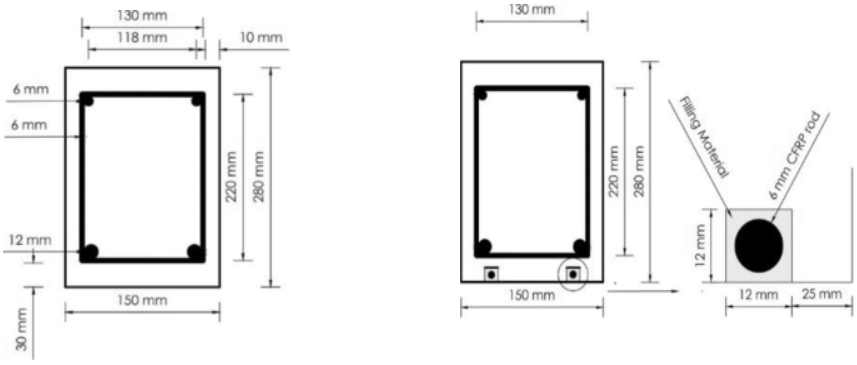

Figure - 2: Un-strengthened and Strengthened Beam Cross Sections with 2, 6 mm FRP Rods,

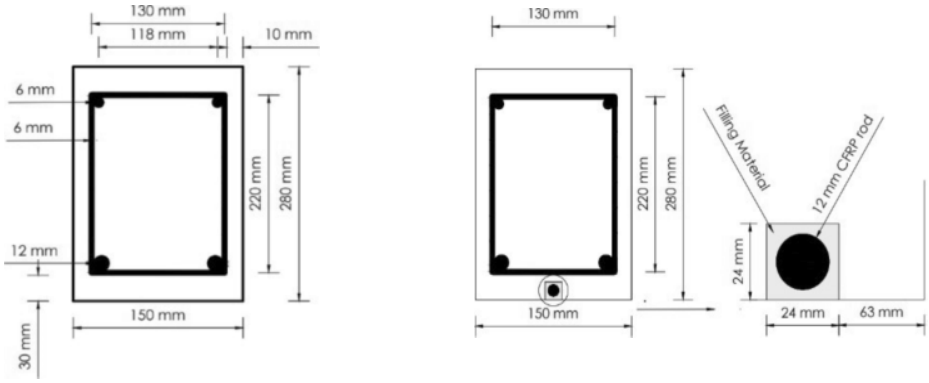

Figure - 3: Un-strengthened and Strengthened Beam Cross Sections with 1, 12 mm FRP Rods,

Table -1 lists the beam specifications used for modelling process in the study.

Table -1**:** Details of Beam Profile

1	Cross Section	150 mm X 280 mm
2	The length of the beam	3000 mm
3	Clear cover	30 mm
4	The distance between the supports on the beam	2800 mm
5	Tensile rebar	2 X 12 mm
6	Compression rebar	2 X 6 mm
7	The length of the main rebar	2940 mm
8	The length of compression rebar	1100 mm on each side
9	The effective depth of the beam	238 mm
10	Stirrups with a 150-mm spacing	Φ 6 mm (130mm X 220mm)
11	Position of load	800 mm from supports

3.1 Material Properties

The mechanical property details of un-strengthened and strengthened beams along with the filling materials is presented in Table-2. Nine out of ten specimens are strengthened with 2Φ6 FRP rods of different lengths of FRP. Al-Mahmoud et. al. (2009) considered four types of variables in the mechanical properties of material and configurations in specimens. This includes concrete strength (conventional VC30 versus high-strength VC60 concrete), two filling materials (Resin and Mortar), different FRP lengths, and different cross-sections of FRP rods (2 Φ6 FRP rods versus 1 Φ12 FRP rod). The compressive and tensile strengths of the adhesive and concrete were measured at 7 and 28 days, respectively

Table - 2: Mechanical Properties and Beam details of Un-strengthened, Strengthened beam and filling material [Al-Mahmoud et. al. (2009)]

Beam Specification	Strength of Concrete	Compressive Strength (MPa)	Tensile Strength (MPa)	Elastic Modulus (GPa)	Number of CFRP Rods	Filling Material	FRP Running Length(mm)
Control beam	VC30	37.4	3.0	30.3	-	-	-
S-C 6 (VC30)	VC30	37.5	3.4	28.4	2Φ6	Epoxy resin	3000
S-C 6 (270-R)	VC30	36.5	3.2	27.9	2Φ6	Epoxy resin	2700
S-C 6 (240-R)	VC30	36.5	3.2	27.9	2Φ6	Epoxy resin	2400
S-C 6 (210-R)	VC30	36.7	3.2	28.1	2Φ6	Epoxy resin	2100
S-C 6 (180-R)	VC30	36.5	3.2	27.9	2Φ6	Epoxy resin	1800
S-C 6 (VC60)	VC60	66.5	5.4	41.3	2Φ6	Epoxy resin	3000
S-C 6 (270 -M)	VC30	38.1	3.3	27.5	2Φ6	Mortar	3000
S-C 12 (VC30)	VC30	35.1	3.4	29.5	1Φ12	Epoxy resin	3000
S-C 12 (VC60)	VC60	67.2	5.6	40.5	1Φ12	Epoxy resin	3000
Epoxy resin	-	83.0	29.5	4.94	-	-	-
Mortar	-	74.6	6.2	31.4	-	-	-

4. Finite Element Modelling

4.1 Material Properties

To capture the effects of concrete compressive strength on the flexural behavior of reinforced concrete beams strengthened with FRP composites, two different concretes, conventional and high-strength concrete denoted by VC30, and VC60, respectively. Table-3 below shows the elastic properties of the two different concretes.

Table - 3: Elastic Properties of Concretes

Concrete Type	Young's Modulus E (GPa)	Compressive Strength σ_c (Mpa)	Poisson's Ratio υ	Density (N/mm^3)
VC30	28.4	37.5	0.2	2.4 E-9
VC60	41.3	66.5	0.2	2.4 E-9

Concrete Damage Plasticity can be used to simulate the plastic behavior of the concrete. The plastic behavior of concrete material is simulated with concrete damage plasticity (concrete compression-tension damage) by using the plastic flow parameters such as compressive strength, Poisson's ratio, angle of dilation, the ratio of biaxial to uniaxial compressive strength, the shear strength ratio between biaxial and triaxial compression, and viscosity. Table-4 lists the flow parameters used in the FE analysis.

Table - 4: Plastic Properties of Concretes

Concrete	Angle of dilation ψ	σ_{b0}/σ_{c0}	K_s	Eccentricity	μ
VC30, VC60	36º	1.16	0.667	0.1	5E-4

For generating concrete damage parameters, prior knowledge of the stress-strain curve is necessary. Since the literature work does not provide any stress-strain relationship, Eurocode 2 is referred to generate the stress-strain relationships and hence the concrete damage parameters were calculated in compression. The paper by Cornelissen et. al. (1986) on Tensile tests and failure analysis of concrete, gives a mathematical model to generate the tensile behavior of concrete using a product of an exponential term and an algebraic term. Thus, the concrete damage parameters were calculated in tension as well. A bilinear elastoplastic model is introduced to model the nonlinear behavior of steel bars. In the proposed model, the steel bars behave as elastic material before the applied stress reaches the yield stress. Thereafter, the plastic deformation occurs continuously with a constantly increasing rate of stress up to the failure state. A brittle fracture model is also introduced to model the FRP composite's response to the applied load as shown in Figure - 4 & 5. In this model, the behavior of FRP rods is assumed to be linear up to the plastic strain. Thereafter, FRP rods lost their resistance instantly.

Table -5: Properties of steel bars and FRP rods

Material	E (GPa)	f_y (MPa)	F_u (MPa)	υ
Steel bars	210	600	700	0.3
FRP rods	146	1875	-	0.22

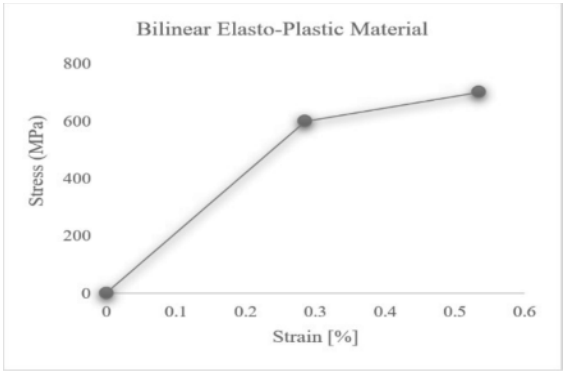

. Figure -4: Bilinear elastoplastic material for steel

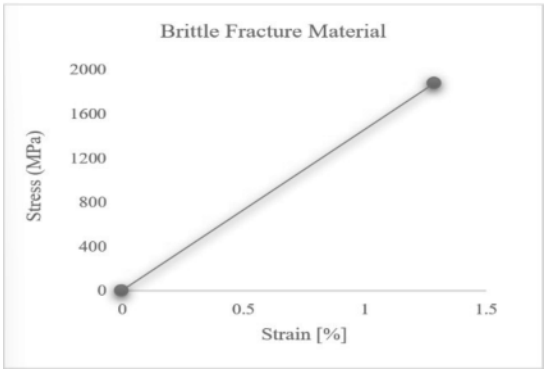

Figure -5: Brittle fracture material for FRP rods

4.2 Element Description

The geometry of specimens, the applied loadings, and the boundary conditions of simulated models are the same in two perpendicular planes. A significant reduction in computational times and efforts makes it more favorable to model the beams using Dynamic explicit analysis. However, we don't need any dynamic effects of loading such as huge kinetic energy or inertial energy; hence, a small smooth loading should be applied.

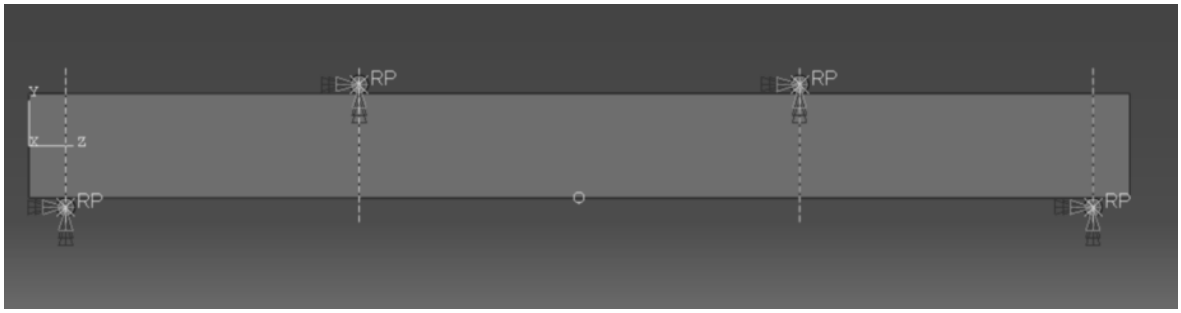

Figure - 6: Finite Element Model of a RC beam with applied loading and boundary conditions

For simulating the analysis, a dynamic step was created to carry out the dynamic explicit analysis for a time duration of 0.2 seconds. Similarly, in the field output, parameters such as displacements, reaction forces and moments, strain values, and damage properties were allotted to be generated in the output. A general interaction property was created for the surfaces in contact. This included the tangential behavior and normal behavior. An embedded body constraint was created to bond the reinforcements with the concrete for which the host region is allocated to the concrete beam, whereas the embedded region includes the reinforcements.

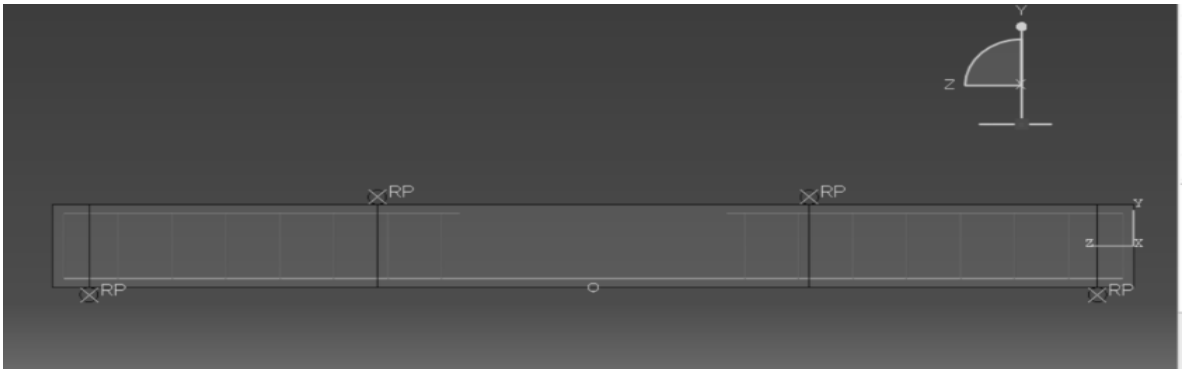

Figure - 7: Assembled view of FE Model of un-strengthened RC beam

The support conditions were applied as fixed support at both ends of the cylindrical rigid roller support. That allowed the beam to move in a Z-direction making it a simply supported beam as in a laboratory. The loading was applied in the form of vertical displacement at the initial step, which was then propagated to the dynamic step where a velocity was applied to the loading support at a speed of 15000 mm/sec for 0.2 seconds using smooth amplitude ramp.

4.3 Meshing the model

To simulate solid materials, three-dimensional eight-node brick elements denoted by C3D8R were used. The C3D8R elements can simulate cracks in tension and compression zones. To simulate structural bars, truss elements can be used. Truss elements with three-dimensional mesh discretization (T3D2)

were used to model structural steel bars. To get the results accurate, an appropriate mesh seed size should be considered, which can be found by repeating the analysis and iterating the process again and again.

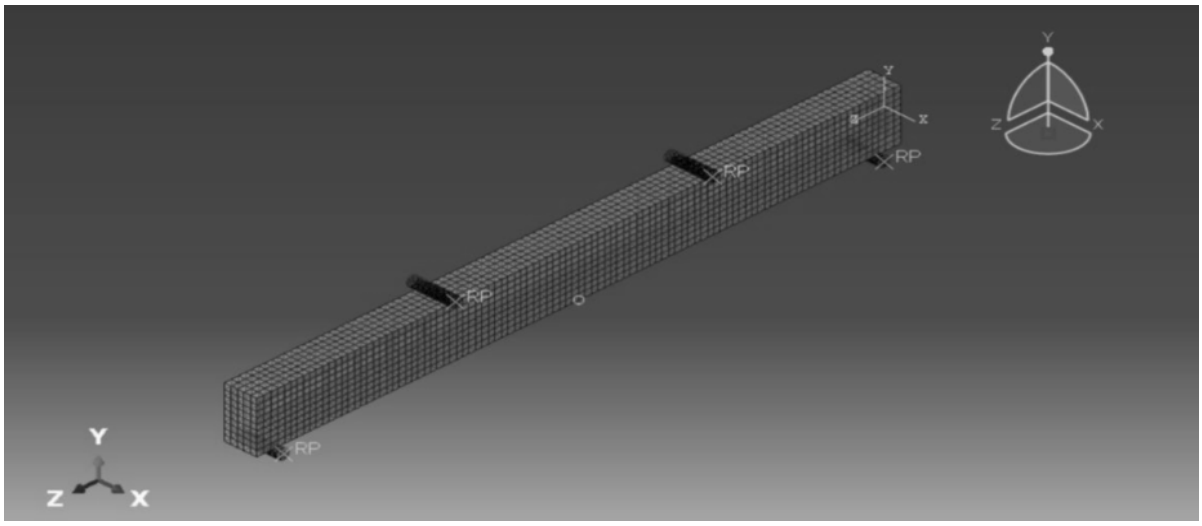

Figure - 8: Meshed reinforced concrete beam along with the parts in assembled form.

5. Finite Element Analysis Result Validation

To model the strengthened beam with NSM FRP rods, it was important to first validate the results obtained from the finite element analysis for the control beam. Therefore, a comparison was made between the obtained results of this study and the experimental results of Al-Mahmoud et. al.'s (2009) work. As can be seen in Table - 6 and Figure - 9, the results of FE analysis were well consistent with the experimental study of Al-Mahmoud et. al. (2009).

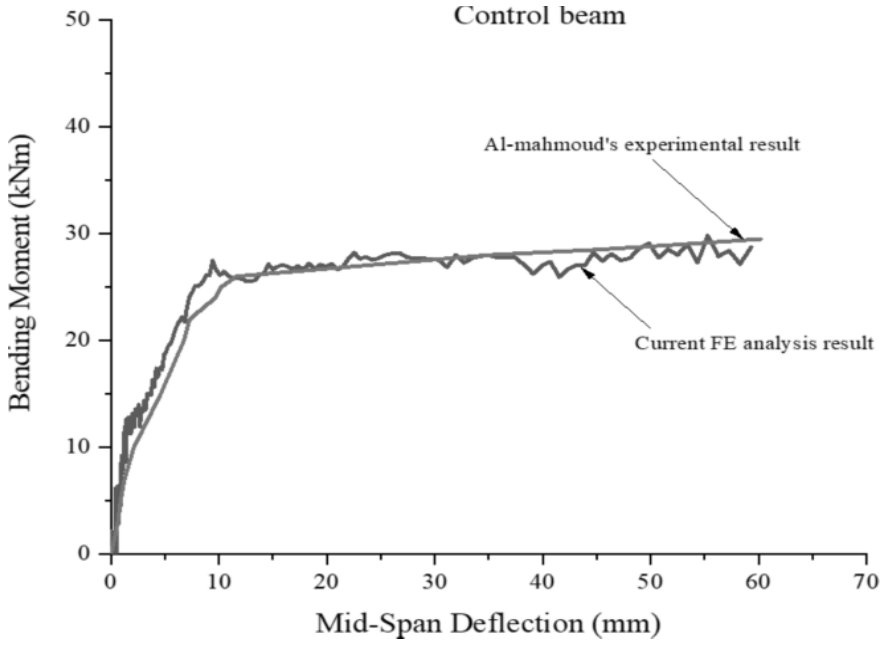

Figure - 9: Bending moment versus Mid-span deflection graph for control beam from FE analysis

Table - 6: Comparison of Finite Element Analysis results with Al-Mahmoud's (2009) experimental results

Beam Property	Al-Mahmoud et. al. work	Current FE Analysis	Difference [%]
Concrete Cracking Moment (kN.m)	7.00	6.51	7
Steel Yielding Moment (kN.m)	28.50	27.80	2.46
Ultimate Bending Moment (kN.m)	29.50	29.80	1.02
Maximum Mid-span Deflection (mm)	60.20	59.32	1.46

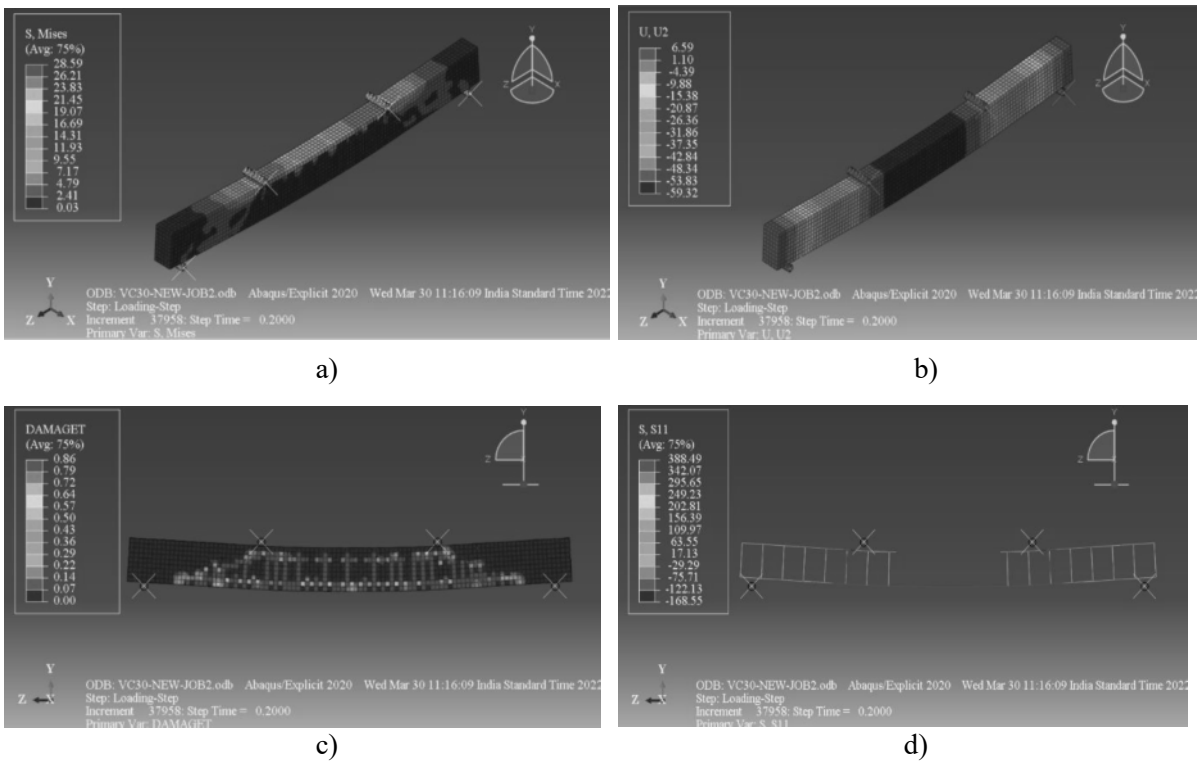

Figure - 10: Contour of a) stress distribution, b) displacement along the beam length, c) DAMAGET distribution, and d) stress distribution along the structural bars

6. NSM FRP Modelling

Once the results for the control beam were validated, nine different beams were modelled and strengthened with FRP rods. The beams S-C 6 (VC30), S-C 6 (270-R), S-C 6 (240-R), S-C 6 (210-R), and S-C 6 (180-R) were modelled with the concrete VC30 and strengthened with two 6 mm-diameter FRP rods which were embedded in the resin and ran along the length of the beam for, 300 cm, 270 cm, 240 cm, 210 cm, and 180 cm, respectively. The purpose of doing so was to compare the behavior of the beams with respect to the strengthening length of FRP rods.

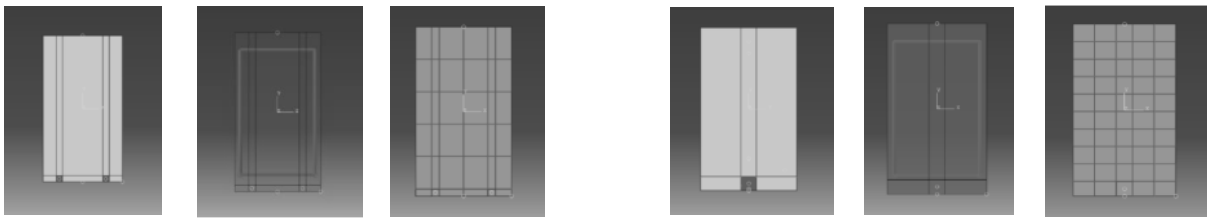

a) b) c) d) e) f)

Figure - 11: Beam strengthened with two 6 mm FRP rods a) with the assembly default b) with reinforcement placement c) with the meshed pattern; Beam strengthened with a single 12 mm FRP rods d) showing assembly default e) showing reinforcement placement f) showing the meshed pattern

Two beams, S-C 12 (VC30) and S-C 12 (VC60) were strengthened with one 12-mm-diameter FRP rod, which was embedded in the epoxy resin and ran along the whole length of the beam. They were modelled with concrete strengths of VC30 and VC60, respectively. One beam, S-C 6 (VC60), was modelled with the concrete VC60 and was strengthened with two 6-mm-diameter FRP rods. The aim of doing so was to compare the behavior of the beams with respect to the FRP cross-section (S-C 6 (VC30) with S-C 12 (VC30)) and (S-C 6 (VC60) with S-C 12 (VC60)). The beam (S-C 6 (270-M)) was modelled with the VC30 concrete and was strengthened with two 6-mm-diameter FRP rods embedded in the mortar that ran along 270 cm length of beam. The reason for doing so was to compare the filling material performance between S-C 6 (270-M) and S-C 6 (270-R). To model the beams with FRP rods, the groove section was tied to the epoxy resin in the modelling process, where the groove section acted as a master surface and epoxy resin surface acted as a slave surface. Then the FRP rod was embedded in the epoxy resin by using an embedded region constraint in the interaction step. This allows the model to make the beam, along with the FRP rod, behave as a single unit.

7. Results and Discussions

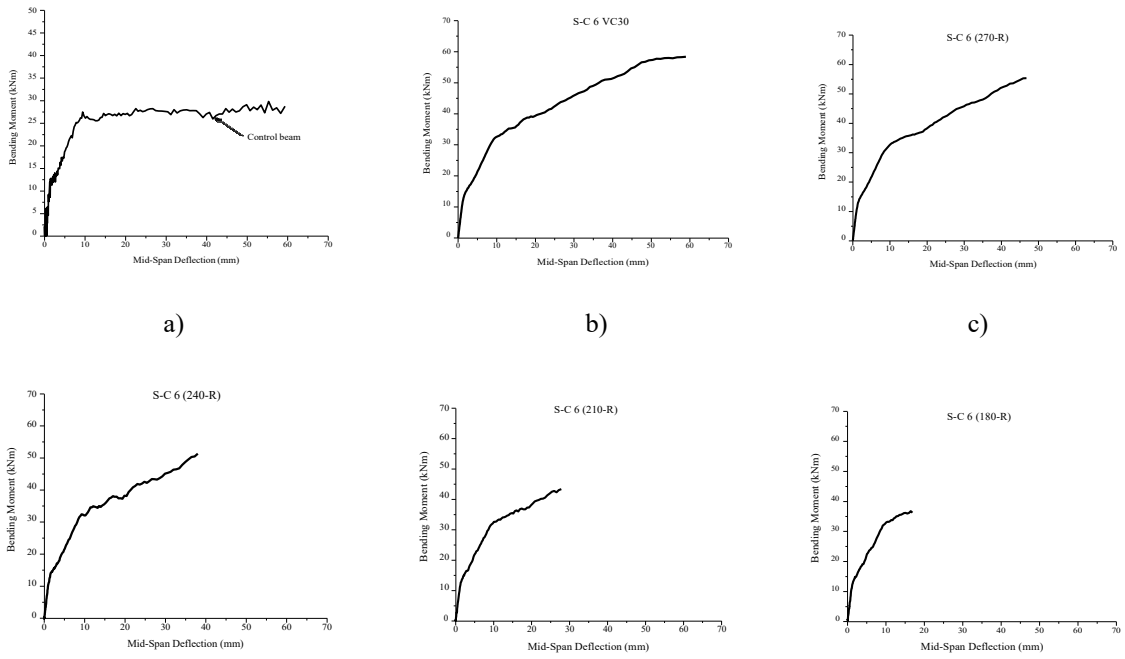

a) b) c) d) e) f)

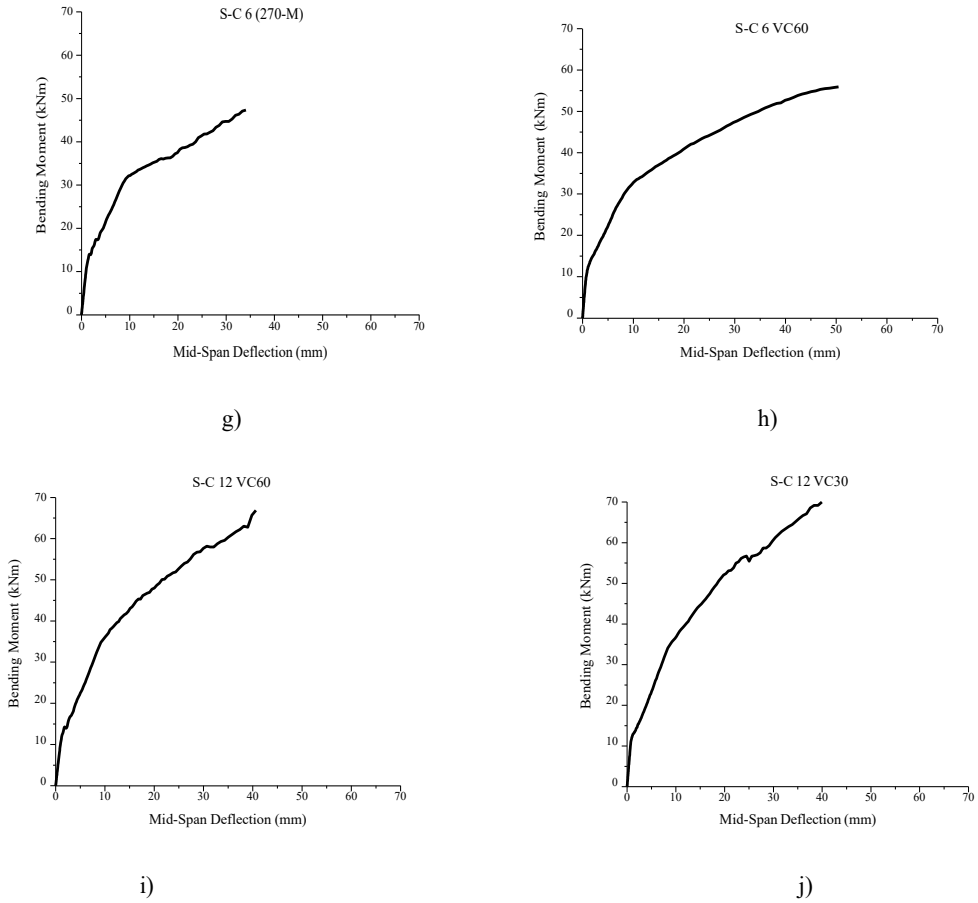

Figure -13: Mid-span deflection versus bending moment for the control beam and nine strengthened beams with NSM FRP rods.

Table - 7: Finite element analysis results of un-strengthened and strengthened beams

Beam	Concrete cracking moment (kN.m)	Steel yielding moment (kN.m)	Ultimate bending moment (kN.m)	Maximum mid-span deflection at failure (mm)
Control Beam	6.51	27.80	29.80	59.32
S-C 6 (VC30)	8.12	35.24	58.98	58.38
S-C 6 (270-R)	7.28	36.54	55.30	46.77
S-C 6 (240-R)	7.69	36.71	51.32	38.02
S-C 6 (210-R)	8.66	37.4	43.43	27.80
S-C 6 (180-R)	7.81	36.14	36.25	16.46
S-C 12 (VC30)	7.60	46.98	66.9	40.63
S-C 12 (VC60)	11.8	44.35	73.3	44.15
S-C 6 (VC60)	12.29	36.25	55.93	50.44
S-C 6 (270-M)	8.64	36.29	47.33	34.08

Figure - 13 represents the mid-span deflection against the bending moment for un-strengthened and strengthened reinforced concrete beams. Similarly, the results on the cracking moment, steel yielding moment, ultimate bending moment, and deflection at failure parameters are reported as in Table-7 based on the finite element analysis done on those models. Because all the beams strengthened by NSM FRP rods were subjected to an increasing positive bending moment, three stages can be distinguished in the mid-span deflection versus maximum bending moment curve. The first stage is an elastic stage, which corresponds to the behavior before concrete cracks.

The graph shows linear behavior up to the elastic range. The second stage is the concrete cracking stage, where cracking starts in the concrete sections of the beam located in the maximum moment zone. At the very beginning of this second stage, the cracks do not cross the filling material because of its higher tensile strength in the case of mortar or its low elastic modulus in the case of epoxy resin. When there is an increase in the load, the cracks become wider and new flexural cracks start. So, at the end of this stage, the moment reaches the value that causes the steel bars to yield. The steel reinforcements up to the second stage have yielded, whereas the FRP rods are still in the elastic range because of their high modulus of elasticity value. The third and last stage is when the beam reaches failure. During these three stages, we can see three different slopes in the curve, as seen in Figure - 13.

7.1 Impact of the Embedded Length of FRP Rods used

The impact of the length of FRP rods used for strengthening was studied with a series of five beams reinforced by two CFRP 6 mm rods embedded in the epoxy resin as filling material. The beams were S-C 6 (VC30), S-C 6 (270-R), S-C 6 (240-R), S-C 6 (210- R), and S-C (180-R). The strengthening length was varied by 300 mm in each case. This was done to create a difference between the beam S-C 6 (VC30) and the beam S-C 6 (270-R) which was that the strengthening was stopped just before the supports. The purpose was to study the behavior of the beam without any FRP rod anchorage effect above the supports. The third, fourth, and fifth beams were strengthened with two 6-mm-diameter FRP rods embedded in the resin and ran along 240 cm, 210 cm, and 180 cm, respectively.

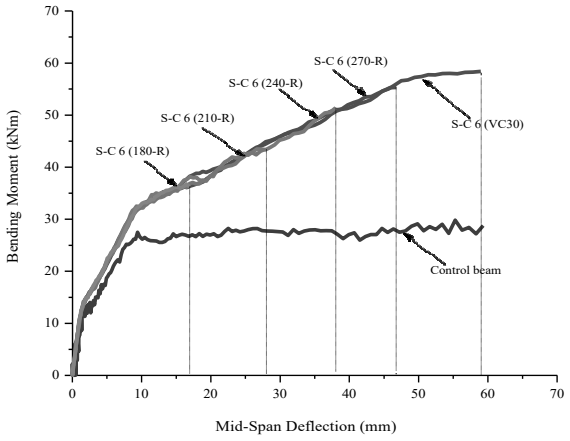

Figure - 14: Comparison of the impact of lengths of FRP rods on strengthened beams

When the loading was applied to beams S-C 6 (VC30), S-C 6 (270-R), S-C 6 (240-R), S-C 6 (210-R), and S-C 6 (180-R), they first showed the elastic stage. After that, steel yielding was reached, but the FRP rods resisted the additional applied load. With the further increase of the applied load, the beam

finally reached an ultimate point and the beams failed. The failure of the S-C 6 (VC30) beam occurred at an ultimate bending moment of 58.98 kN.m, 97.92 % more compared to the control beam while the failure of the S-C 6 (270-R) beam occurred at an ultimate bending moment of 55.30 kN m with an increase of 85.57% in the failure load as reported in Table - 7.

The difference in the ultimate bending moment can be because the FRP rods, provided in the first beam ran all along the beam length, providing the anchoring length that was not there in the other beams that followed. The beams S-C 6(240-R), S-C 6 (210-R), and S-C 6 (180-R) reached an ultimate bending moment of 51.32 kN.m, 43.43 kN.m, and 36.25 kN.m, respectively, which showed an increase of 72.21 %, 45.74 %, and 21.64 %, respectively. This shows that by providing a greater length of FRP rods for strengthening, the ultimate capacity of beams can be increased to a greater extent. Also, the length of the FRP rod greatly affected the ultimate deflection at the failure Compared to the control beam, which had reported a maximum deflection of 59.32 mm, the beams other than S-C 6 (VC30) reported a huge declination in the deflection value at failure. S-C 6 (270-R), S-C 6(240-R), S-C 6 (210-R), and S-C 6 (180-R) showed a maximum deflection of 46.77 mm, 38.02 mm, 27.80 mm, and 16.46 mm, respectively. This also suggests that with a shorter FRP rod length, there is a huge reduction in the maximum deflection that the beam can reach before the failure. It can be said that 300 mm more length of the FRP rods led to about a 12.6 mm increase in deflection before failure, as seen in Figure-14. Hence, the efficiency of strengthening the reinforced concrete beam increased by a huge amount with an increase in the embedded length of FRP rods.

7.2 Impact of Filling Material used

To study the impact of filling material on the cracking behavior and the ultimate beam strength, S-C 6 (270-R), and S-C 6 (270-M) beams were modelled. These beams had the same strengthening length of 2700 mm, the same FRP rod section, i.e., two 6-mm FRP rods, and the same concrete strength (VC30). Two different filling materials, epoxy resin, and mortar were used and their impacts were analyzed.

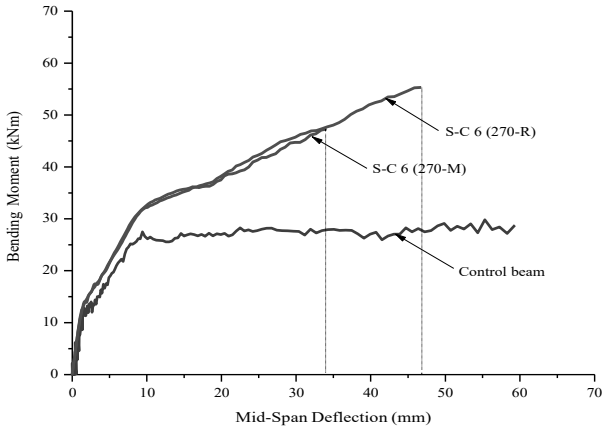

Figure - 15: Comparison of the impact of Filling material on strengthened beams

Failure of the S-C 6 (270-M) beam occurred at an ultimate bending moment of 47.33 kN.m, nearly 59 % more than the control beam. Whereas, the ultimate bending moment at failure was 55.30 kN.m for beam S-C 6 (270-R), nearly 85 % more than that of the control beam. This shows that when shifted from mortar as a filling material to epoxy resin, the ultimate bending moment increased by nearly 8 kN m, which is by nearly 27 % as seen in fig. 15. This means that the FRP rods embedded in the resin formed a better bond with the concrete than the ones embedded in the mortar.

7.3 Impact of FRP Rod Section used

The impact of the FRP rod section was studied on beams S-C 6 (VC30), S-C 12 (VC30), S-C 6 (VC60), and S-C 12 (VC60). The beams S-C 6 (VC30) and S-C 6 (VC60) were modelled by strengthening with two 6-mm-diameter FRP rods embedded in the epoxy resin, which ran throughout the beam length. The remaining two beams, S-C 12 (VC30) and S-C 12 (VC60) were modelled by strengthening with one 12-mm-diameter FRP rod embedded in the epoxy resin.

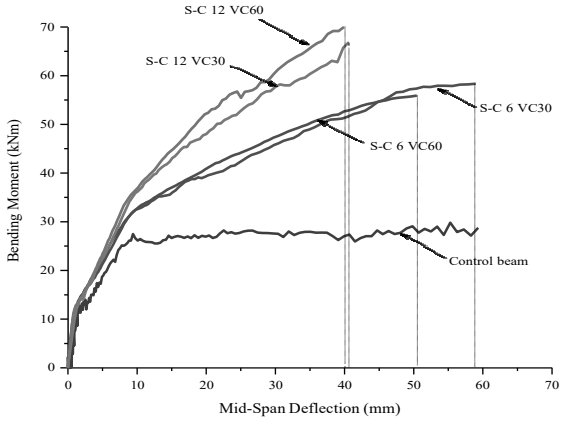

Figure - 16: Comparison of the impact of FRP rods section on strengthened beams

The difference in ultimate carrying capacity for S-C 6 (VC30) and S-C 12 (VC30) beams or for S-C 6 (VC60) and S-C 12 (VC60) beams can be seen in fig. 16. Due to the larger cross-section of one 12-mm CFRP rod compared to the cross-section of two 6-mm CFRP rods, the beam showed a greater ultimate carrying capacity as the section made the beam stiffer. The increase in stiffness observed with S-C 12 (VC30) and S-C 12 (VC60) beams can also be verified from fig. 16 since it reduced the maximum mid-span deflection value at ultimate load capacity. The failure of the S-C 12 (VC30) beam occurred at 66.9 kN.m, 124% more than of ultimate load of the control beam compared to the S-C 6 (VC30) beam, where the failure occurred at 58.98 kN.m, nearly 98 % more than the ultimate load of control beam.

Providing a greater cross-section resulted in about 26 % more ultimate load-carrying capacity of the beam. Similarly, the failure of the S-C 12 (VC60) beam occurred at 73.3 kN.m, 146% more than the ultimate load of the control beam compared to the S-C 6 (VC60) beam, where the failure occurred at nearly 88 % more than the ultimate load of the control beam. The ultimate load of the S-C 12 (VC60) beam was higher than that of the S-C 6 (VC60) beam by nearly 17 kN.m, 58 %. Therefore, this proves the fact that in the case of strengthened beams, the difference in stiffness provided by one 12-mm FRP rod compared to two 6-mm CFRP rods greatly increased the ultimate load-carrying capacity but this came at the cost of ductility as the ultimate deflection got restricted due to stiffness.

7.4 Impact of Concrete Strength used

S-C 6 (VC30) and S-C 6 (VC60) beams can be analyzed to study the effect of concrete strength on the flexural capacity of the beams. As reported in Table-7, these two beams had almost the same ultimate moment, even though the cracking moment of concrete value was different.

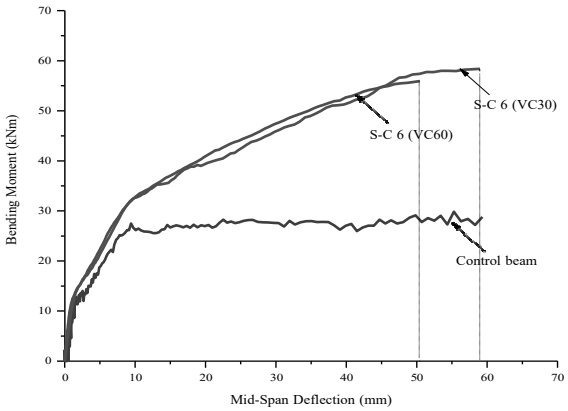

Figure - 17: Comparison of the impact of concrete strength on strengthened beams

The ultimate bending moments for S-C 6 (VC30) and S-C 6 (VC60) were 58.98 and 55.93, respectively. The value varied by a value of nearly 3 kN.m (nearly 5 %). Thus, the concrete strength has very little influence on the ultimate load-carrying capacity of the strengthened beam. The S-C 12 (VC60) beam exhibited a higher ultimate moment failure at 73.3 kN m compared to the S-C 12 (VC30) beam, which failed at 66.9 kN m. This could be due to its higher compressive strength. In conclusion, the concrete strength is not as important a parameter as the three other parameters influencing the ultimate beam strength.

8. CONCLUSIONS

This study, based on the results of the analysis performed draws multiple conclusions. The finite element analysis result showed a good consistency with the experimental results obtained through Al-Mahmoud et. al.'s work with a maximum deviation of 7%. The bending moment versus mid-span deflection curve for all strengthened beams with FRP rods showed the same trend which was a tri-linear response defined by concrete cracking, steel yielding, and ultimate bending stages lasting till the failure. The flexural capacity of reinforced concrete beams with NSM FRP rods significantly increased in comparison to those of the control beam while the mid-span deflections of strengthened beams at failure mainly decreased compared to the control beam. The flexural strength increased by maximum of 126% for VC30 concrete and 146% for VC60 concrete. The ultimate bending moment of beams increased with an increase in length of FRP rods used. The flexural strength increased by nearly 98% when the FRP rods ran all along the beam length. Providing smaller length of FRP rods significantly reduced the mid-span deflection at failure. The deflection value reduced by nearly 72% when 180 cm long FRP rods were provided. The NSM technique using FRP rods turns out to be a very effective technique in enhancing the flexural strength of reinforced concrete beams for both type of filling materials, epoxy resin and mortar. The flexural strength increased by 86% for epoxy resin whereas 59% for mortar. The ultimate bending moment of beams with 1Φ12 FRP rod was higher than 2Φ6 FRP rods since a greater area provided greater stiffness to the beam resulting in about 26% more strength, but the maximum mid-span deflection value decreased. The concrete strength showed small influence on the load-carrying capacity of the strengthened beam as their flexural strength varied by a small value.

References

1. Abdzaid, H. M., & Kamonna, H. H. (2019). Flexural strengthening of continuous reinforced concrete beams with near-surface-mounted reinforcement. *Practice Periodical on Structural Design and Construction, 24*(3), 04019014.
2. Al-Mahmoud F, Castel A, François R, Tourneur C. Anchorage and tension-stiffening effect between near-surface-mounted carbon fibre-reinforcement polymer rods and concrete. Paper presented at 2nd international symposium on advances in concrete through science and engineering, Quebec City, Canada, 11–13 September; 2006.
3. Al-Mahmoud F, Castel A, François R, Tourneur C. Effect of surface pre-conditioning on bond of carbon fiber reinforced polymer rods to concrete. Cem Concr Compos 2007;29(9):677–89. 1.
4. Al-Mahmoud, F., Castel, A., François, R., & Tourneur, C. (2009). Strengthening of RC members with near-surface mounted CFRP rods. *Composite structures, 91*(2), 138-147.
5. Ceroni, F. (2010). Experimental performances of RC beams strengthened with FRP materials. Construction and Building materials, 24(9), 1547-1559.
6. De Lorenzis, L., & Nanni, A. (2002). Bond between near-surface mounted fiber-reinforced polymer rods and concrete in structural strengthening. Structural Journal, 99(2), 123-132.
7. De Lorenzis, L., & Nanni, A. (2001). Shear strengthening of reinforced concrete beams with near-surface mounted fiber-reinforced polymer rods. Structural Journal, 98(1), 60-68.
8. De Lorenzis, L., Nanni, A., & La Tegola, A. (2000, May). Strengthening of reinforced concrete structures with near surface mounted FRP rods. In International meeting on composite materials, PLAST (pp. 9-11).
9. Eurocode 2
10. Hassan, T., & Rizkalla, S. (2004). Bond mechanism of NSM FRP bars for flexural strengthening of concrete structures. ACI Structural journal, 101(6), 830-839.
11. Panahi, M., & Izadinia, M. (2018). A parametric study on the flexural strengthening of reinforced concrete beams with near surface mounted FRP bars. Civil Engineering Journal, 4(8), 1917-1929.
12. Reinhardt, H. W., Cornelissen, H. A., & Hordijk, D. A. (1986). Tensile tests and failure analysis of concrete. Journal of structural engineering, 112(11), 2462-2477.
13. Seracino, R., Jones, N. M., Ali, M. S., Page, M. W., & Oehlers, D. J. (2007). Bond strength of near-surface mounted FRP strip-to-concrete joints. Journal of Composites for Construction, 11(4), 401-409.
14. Sharaky, I. A., Torres, L., Comas, J., & Barris, C. (2014). Flexural response of reinforced concrete (RC) beams strengthened with near surface mounted (NSM) fibre reinforced polymer (FRP) bars. Composite Structures, 109, 8-22.
15. Zhang, H., He, L., & Li, G. (2015). Bond failure performances between near-surface mounted FRP bars and concrete for flexural strengthening concrete structures. Engineering Failure Analysis, 56, 39-50.